

Modeling of Holographic Imaging of Volume Object using Modified Covariance Method

MUJAHID AL-AZZO

Department of Electronics Engineering
Faculty of Electronics Engineering-Ninevah University
Mosul - IRAQ
Email: mujaz1@hotmail.com

Abstract: A high resolution modified covariance method is applied to model an ultrasonic holographic imaging (detection) of volume objects. The results demonstrate the enhanced performance capability of the combination of modified covariance and holographic techniques. The results are compared with the traditional, Fourier transform, method. The performance is investigated for different values of some parameters of the object under imaging process.

Keywords: Modified covariance method, spectral estimation, holographic technique.

1. Introduction

The estimation of the number of harmonics, and their amplitudes and frequencies, from the data, is a problem frequently encountered in several signal processing applications, such as in estimating the direction of arrival (DOA) of narrow-band source signals, radio and microwave communication, underwater acoustics, etc.

The problem under consideration concerns information extraction from measurements using spatially synthetic aperture scanning of ultrasonic transmit/receive transducer.

The classical (traditional) power spectral estimation methods, also known as non-parametric method, are based on Fourier transformation (FT) of the measured data. This method is computationally efficient, but it suffers from sidelobes, and limited resolution [1]. Resolution is a minimum separation between the parts of the object to be resolved. Therefore it is required to look for another method that has no or less sidelobes and better resolution. A modern, also known as parametric methods, contribute in solving the limited resolution. A modified covariance method is one of these. It is a high resolution and stable method, so it has been widely used in many applications [2, 3]. It generates frequency component estimates for a signal based on linear prediction modeling and minimization of the forward and backward errors in linear predictors.

The interest in acoustic waves for detection and imaging stems from its properties as highly coherent waves [4]. The ability of ultrasound waves to penetrate many materials that are optically opaque makes them very important for detecting

and imaging targets that cannot be imaged by light waves [4],[5].

The object under consideration is either transmitting the ultrasonic acoustic waves or illuminated by ultrasound waves, and the received (or reflected (backscattered)) waves are sampled and recorded. The recording of the signal includes its amplitude and phase. Holography was initiated as an interferometric technique for recording the amplitude and phase of a coherent wave, whether it is electromagnetic or acoustic wave. A recording of this interference pattern is called a hologram, a term coined by Dennis Gabor in 1948 [6]. Holography has received considerable attention since more than three decades. It has been applied in the fields of optical, acoustical, and microwave radiations [7], [8], [9],[10],[11]. The holographic soundfield imaging technique combines the ultrasonic wave with the holographic interferometry.

The holographic data are modeled as an autoregressive (AR) process where the prediction coefficients are calculated by the modified covariance method. The combination of high resolution and holographic techniques improves the performance of the problem [12]. The use of holography enables improvement of the signal-to-noise ratio by coherently cumulating the acoustic field on the ultrasonic transducers when scanning the field [13]. The imaging process consists of two steps: the recording of the hologram and the image reconstruction of the object.

2. Principle of Holography

2.1 Field Analysis at Recording Aperture [7],[10],[14]

For simplicity, the analysis is given for the plane object, and then in the second subsection (2.2 subsection) a modification on the analysis is made to be suitable for the volume object.

The object, under imaging (detection) process, is assumed to have a field distribution $D(p)$. This distribution propagates to the recording axis X (called a hologram) where it produces the field distribution $S(x)$, given by:

$$S(x) = \frac{B}{Z_o \lambda} \int_p D(p) \exp(jkr(p, x)) dp \quad (1)$$

This is the paraxial approximation to the Huygens-Fresnel principles. B is a complex constant, k is a propagation constant (wave number), Z_o is the distance between the object and recording (observation) planes, and r is the distance from a typical point on the object to a typical point on the recording axis X . r is given as:

$$r(p, x) = \sqrt{Z_o^2 + (x - p)^2} \quad (2)$$

According to a paraxial approximation, where

$$((x - p)^2 / Z_o^2) \ll 1 \quad (3)$$

Then (2) is written as:

$$r(p, x) = Z_o + \frac{(x - p)^2}{2Z_o} - \frac{(x - p)^4}{8Z_o^3} + \dots \quad (4)$$

In Fresnel region, r can be approximated by the first two terms of (4), hence

$$r(p, x) = Z_o + \frac{x^2}{2Z_o} + \frac{p^2}{2Z_o} - \frac{px}{Z_o} \quad (5)$$

Substituting (5) into (1) yields

$$S(x) = B_1 \exp\left(\frac{jkx^2}{2Z_o}\right) \int_p D(p) \exp\left(\frac{jkp^2}{2Z_o}\right) \exp\left(-\frac{jkxp}{Z_o}\right) dp \quad (6)$$

where B_1 is a complex constant resulting from (1) and (5).

2.2 The Field of a Volume Object at Recording Aperture

A volume object is an object that its parts are at different distances from the recording axis (hologram axis), so we have more than one value of Z_o , each one belongs to corresponding part of the object. For simplicity we assume that the object consists of two parts, one of them is located at a distance Z_1 from the recording plane and the other part is located at a distance Z_2 from the recording plane.

The object, under imaging (detection) process, is assumed to have a field distribution $D(p_1)$ corresponding to Z_1 and $D(p_2)$ corresponding to Z_2 . Hence the field distribution $S_1(x)$ that corresponds to Z_1 is given as

$$S_1(x) = \frac{B}{(Z_1)\lambda} \int_{p_1} D(p_1) \exp(jkr_1(p_1, x)) dp_1 \quad (7-a)$$

and the field distribution $S_2(x)$ that corresponds to Z_2 is

$$S_2(x) = \frac{B}{(Z_2)\lambda} \int_{p_2} D(p_2) \exp(jkr_2(p_2, x)) dp_2 \quad (7-b)$$

where

$$r_1(p_1, x) = \sqrt{(Z_1)^2 + (x - p_1)^2} \quad (8-a)$$

and

$$r_2(p_2, x) = \sqrt{(Z_2)^2 + (x - p_2)^2} \quad (8-b)$$

Then the total field at the recording axis X is

$$S(x) = S_1(x) + S_2(x) \quad (9)$$

Following the same procedure as in subsection 2.1, the fields are

$$S_1(x) = B_1 \exp\left(\frac{jkx^2}{2(Z_1)}\right) \int_{p_1} D(p_1) \exp\left(\frac{jkp_1^2}{2(Z_1)}\right) \exp\left(-\frac{jkxp_1}{Z_1}\right) dp_1 \quad (10-a)$$

and

$$S_2(x) = B_2 \exp\left(\frac{jkx^2}{2(Z_2)}\right) \int_{p_2} D(p_2) \exp\left(\frac{jkp_2^2}{2(Z_2)}\right) \exp\left(-\frac{jkxp_2}{Z_2}\right) dp_2$$

(10-b)

and the total fields will be

$$S(x) = S_1(x) + S_2(x) \quad (11)$$

2.3 Image Reconstruction

For simplicity, image reconstruction of a plane object is discussed, and then an extension to an image reconstruction of a volume object is given. An image can be extracted from the recorded hologram $h(x)$ through its multiplication by the focusing phase factor $\exp(-\frac{jkx^2}{2Z_o})$ and subsequent

application of either Fourier transformation FT (a classical method) [17] or one of the modern high resolution spectral analysis, such as the modified covariance method.

For a volume object and as discussed above, the image reconstruction is performed by multiplying the hologram equation (Equ.11) with a phase factor $\exp(-\frac{jkx^2}{2Z_i})$, $i=1,2,\dots,M$; where M is

the number of object's parts that are located at different depths, and then applying either Fourier transformation FT (a classical method) [17] or one of the modern high resolution spectral analysis, such as the modified covariance method. So by choosing the value of Z_i in the phase factor, an image will be focused at Z_i from the hologram aperture. Hence, the holographic imaging system can produce different images at different planes along the depth of the volume object using only one hologram recording.

3. Modified Covariance Method

The derivation of this method can also be found in many references [15,16]. The modified covariance method for estimating the autoregressive parameters of order p (AR(p)) can be viewed also as least-squares method, based on the minimization of the forward and backward errors in linear predictors. The hologram $S(x)$, or $h(x)$ is sampled, and the distance between each two samples is Δx . The number of samples is N . The resultant hologram is then $h(n)$; $n=0,1,\dots,N-1$. To derive the estimator, let us consider the forward and backward linear prediction estimates of order p , given as

$$\hat{h}(n) = -\sum_{k=1}^p a(k)h(n-k) \quad (12)$$

$$\hat{h}(n) = -\sum_{k=1}^p a^*(k)h(n+k) \quad (13)$$

Where $a(k)$'s are the AR filter parameters. In either case the minimum prediction error power is just the white noise variance σ^2 . The modified covariance method estimates the AR parameters by minimizing the average of the estimated forward and backward prediction error powers, or

$$\hat{\rho} = \frac{1}{2} \left(\hat{\rho}^f + \hat{\rho}^b \right) \quad (14)$$

where

$$\hat{\rho}^f = \frac{1}{N-p} \sum_{n=p}^{N-1} \left| h(n) + \sum_{k=1}^p a(k)h(n-k) \right|^2 \quad (15)$$

$$\hat{\rho}^b = \frac{1}{N-p} \sum_{n=0}^{N-1-p} \left| h(n) + \sum_{k=1}^p a^*(k)h(n+k) \right|^2$$

A least-square solution is used for minimization of (9). The result is [15, 16]

$$\begin{bmatrix} c_{hh}(1,1) & c_{hh}(1,2) & \dots & c_{hh}(1,p) \\ c_{hh}(2,1) & c_{hh}(2,2) & \dots & c_{hh}(2,p) \\ \vdots & \vdots & \ddots & \vdots \\ c_{hh}(p,1) & c_{hh}(p,2) & \dots & c_{hh}(p,p) \end{bmatrix} \begin{bmatrix} \hat{a}(1) \\ \hat{a}(2) \\ \vdots \\ \hat{a}(p) \end{bmatrix} = - \begin{bmatrix} c_{hh}(1,0) \\ c_{hh}(2,0) \\ \vdots \\ c_{hh}(p,0) \end{bmatrix} \quad (16)$$

where

$$c_{hh}(i,j) = \frac{1}{2(N-p)} \left(\sum_{n=p}^{N-1} h^*(n-i)h(n-j) + \sum_{n=0}^{N-p-1} h(n+i)h^*(n+j) \right) \quad (17)$$

Solving (16) will give the values of $a(k)$, $k=1,2,\dots,p$. Then the power spectral density can be estimated using the values of $a(k)$, $k=1,2,\dots,p$.

The estimate of the white noise variance is

$$\hat{\sigma}^2 = c_{hh}(0,0) + \sum_{k=1}^p \hat{a}(k)c_{hh}(0,k) \quad (18)$$

The power spectral density is:

$$P_{hh}(f) = \frac{\hat{\sigma}^2}{\left| 1 + \sum_{k=1}^p \hat{a}(k) e^{-j2\pi f k} \right|^2} \quad (19)$$

The advantages of the modified covariance method for estimating the parameters of the AR model are: 1- it yields statistically stable spectral estimates with high frequency resolution [3,15], 2- the usual shifting of the peaks of an AR spectral estimate from the true frequency locations due to additive observation appears to be less pronounced for many of the other AR spectral estimators, and 3- spectral line splitting in which a single sinusoidal component gives rise to two distinct spectral peaks has never been observed [15].

4. Simulation Results

A test object consists of two points, two ultrasonic transmitting sources (transducers) of about 1cm width used. The separation between the transducers is 3 cm. One of these transducers is located at $Z_i=Z_1=45$ cm, while the other at $Z_i=Z_2=30$ cm. This means that the object depth is 15 cm. The other parameters were $\lambda=0.8$ cm and sampling interval is $\Delta x=0.6$ cm. The transmitted ultrasonic waves is impinging the receiving transducer. The receiving transducer scans the hologram aperture to record the received signal at uniformly spaced (Δx) positions. The total number of samples is N . The modified covariance method is used.

The results of modified covariance method is shown in figures 1 and 2. Figure 1 shows an image obtained by focusing at distance 45cm from the hologram aperture. The higher peak corresponds to the source at $Z_i=Z_1=45$ cm, while the lower peak corresponds to the defocused image of the source that is located at $Z_i=Z_2=30$ cm from the hologram aperture. Figure 2 shows the inverse case.

We proposed that the acceptable range of the absolute difference between the focused and defocused peaks is approximately between 3dB and 10dB.

Table 1 shows the performance of modified covariance method for some parameters of the object.

It is worthwhile to mention that the resolution formula for the Fourier transform is given by:

$$\sigma = \frac{\lambda Z_o}{a} \quad (20)$$

where a represents half of the aperture length, and is given as:

$$a = \frac{(N-1)\Delta x}{2} \quad (21)$$

The remaining parameters of Table 1 are:

d: depth (axial depth) of object's parts.

s: separation (lateral separation) of object's parts.

It is clear from the table that as the separation, s , decreases, the aperture length, $2a$, should be increased. However, when s is decreased by 14%, the corresponding increase in $2a$ is only 10% as it is clear from first and second rows of the table. Also, when the depth, d , is decreased by 25%, and the separation, s , by 14%, then this requires that the aperture length, $2a$, to be increased only by 20% as it is clear from first and third rows of the table.

5. Conclusion

It is demonstrated that the modified covariance method can be used to image and detect a volume object of deeply separated points, and to find the required parameter such as the amplitude and to decrease the effect of sidelobes. Modified covariance method outperforms the FT method.

References

- [1] S.L. Marple, *Digital Spectral Analysis with applications*, Englewood Cliffs, NJ: Prentice – Hall, 1987.
- [2] S. Cavalcanti, L. Chiari, S. Severi, G. Avanzolini, G. Enzmann, C. Lamberti, Parametric analysis of heart rate variability during hemodialysis, *International Journal of Bio-Medical Computing*, vol.42, No.3, Aug. 1996, p.215-224.
- [3] A. vizinho, L.R. Wyatt, Evaluation of the use of the modified-covariance method in HF radar ocean measurement, *IEEE Journal of Ocean Engineering*, vol.26, No.4, p832-840, Oct. 2001.
- [4] *Proc. IEEE, Special Issue on Acoustic imaging"*, vol.67, No.4, p.452-675 Apr. 1979.
- [5] V. A. Deason, K.L. Telschow, S.M. Watson, Imaging of acoustic waves in sand", *Proc. of SPIE*, vol.5191, p 1-7, Nov.2003.
- [6] J.W. Goodman, *Introduction to Fourier Optics*, Third Edition, Roberts & Company Publisher, 2004.
- [7] Grilli, S., Ferraro, P., De Nicola, S. Finizio, A., Pierattini, G., Meucci, R., Whole optical

wavefields reconstruction by Digital holography, *Optics Express* vol. 9, No. 6, p 294-302, 2001.

[8] A.Greve, D.Morris, Repetitive radio Reflector surface deformation, *IEEE Trans. Antennas & Propagation*, vol.53, no.6, p 2123-2126, June 2005.

[9] G.F.Garlick, J.O.Shelby, Detector in ultrasonic holography, *J.Acoustic Soc.Am.*, vol. 114, No.6, p 2995 March 2004.

[10] A.P. Anderson, Microwave holography, *IEE Proc.*, vol.129, part H, Aug.1982.

[11] K. H. Sayidmarie, A. P. Anderson, J.C. Bennet, Digital in-line holographic techniques for long wavelength imaging, *Proc. IEE*, vol.129, part h, No.4, Aug. 1982. p 211-220.

[12] D. Carl, B. Kemper, and G. VonBally, Parameter-optimized digital holographic microscope for high- resolution living cell

analysis", *Applied Optics* 43 (36), 2004, p 6536-6544.

[13] P.Roux, Dieder Casserau, A. Roux, "A high resolution algorithm for wave number estimation using holographic array processing", *J.Acoustic Soc.Am.*, vol.115, no.3, March 2004.

[14] V.Toal , *Introduction to Holography* , CRC Press , Taylor & Francis Group , 2012.

[15] S. M. Kay *Modern spectral estimation*, Prentice Hall, New Jersey, 1988.

[16] T. K. Moon, W. C. Stirling, *Mathematical methods and algorithms for signal processing*, Prentice Hall, New Jersey, 2000.

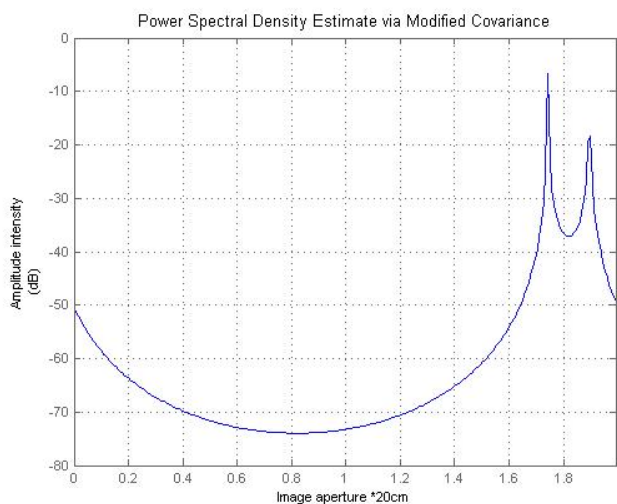


Fig.1 Reconstructed image using modified covariance method. Focusing distance is $Z_1=45$ cm

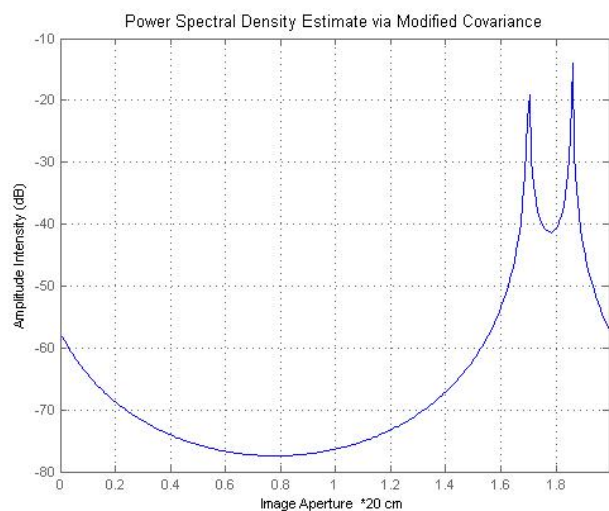


Fig.2 Reconstructed image using modified covariance method. Focusing distance is $Z_2=30$ cm.

Table 1 A comparison of the performance of modified covariance method

	d (cm)	s (cm)	2a (cm)
1	20	3.5	5
2	20	3	5.5
3	15	3	6
4	15	2.5	6
5	10	2.5	6